Bioresource Technology 102 (2011) 10280–10285

Contents lists available at SciVerse ScienceDirect

Bioresource Technology

journal homepage: www.elsevier.com/locate/biortech

Basic dye adsorption onto an agro-based waste material – Sesame hull (*Sesamum indicum* L.)

Yanfang Feng [a,c], Fan Yang [a], Yongqian Wang [a,c], Li Ma [a], Yonghong Wu [a,*], Philip G. Kerr [b], Linzhang Yang [a,*]

[a] State Key Laboratory of Soil and Sustainable Agriculture, Institute of Soil Science, Chinese Academy of Sciences, No. 71, East Beijing Rd., Nanjing, Jiangsu 210008, PR China
[b] School of Biomedical Sciences, Charles Sturt University, Wagga Wagga, NSW 2678, Australia
[c] Graduate University of Chinese Academy of Sciences, Beijing 100049, PR China

ARTICLE INFO

Article history:
Received 28 April 2011
Received in revised form 17 August 2011
Accepted 21 August 2011
Available online 27 August 2011

Keywords:
Methylene blue
Biosorption
Sesame hull (*Sesamum indicum* L.)

ABSTRACT

The aim of this project was to establish an economical and environmentally benign biotechnology for removing methylene blue (MB) from wastewater. The adsorption process of MB onto abandoned sesame hull (*Sesamum indicum* L.) (SH) was investigated in a batch system. The results showed that a wide range of pH (3.54–10.50) was favorable for the adsorption of MB onto SH. The Langmuir model displayed the best fit for the isothermal data. The exothermic adsorption process fits a pseudo-second-order kinetic model. The maximum monolayer adsorption capacity (359.88 mg g^{-1}) was higher than most previously investigated low-cost bioadsorbents (e.g., peanut hull, wheat straw, etc.). This study indicated that sesame hull is a promising, unconventional, affordable and environmentally friendly bio-measure that is easily deployed for removing high levels of MB from wastewater.

1. Introduction

Synthetic dyes are widely used throughout the world. The annual production is over 7×10^5 tons (Murugesan et al., 2007). As a result, considerable amounts of synthetic dyes from textile, leather, food processing, cosmetics, paper, and dye manufacturing industries are discharged into the environment every year (Sharma et al., 2010). In the case of the textile industry alone, more than 1.5×10^8 m^3 of colored effluents are discharged annually (Ip et al., 2010). Once colored wastes (e.g., synthetic dyes) enter the waters, the transmission of sunlight through the water can lead to reduced photosynthetic activity by macrophytes. In addition, synthetic dyes may release toxic compounds, affecting both human and aquatic life (Bhattacharyya and Sharma, 2005). Thus, it is good practice to remove synthetic dyes before they enter downstream bodies of water.

Among synthetic dyes, methylene blue (MB) is a heterocyclic aromatic compound that has significant adverse impacts on flora, fauna and aquatic ecosystems (Ghosh and Bhattacharyya, 2002). Moreover, MB is often used as a model (indicator) for identifying the adsorption capacity of adsorbents (Bestani et al., 2008). Thus, investigating the removal of MB from wastewater is both practical and significant.

The common removal (decolorization) measures for synthetic dyes are summarized as follows: coagulation, flocculation, microbiological or enzymatic decomposition, adsorption, membrane filtration, ion-exchange, oxidation and advanced oxidation (Crini, 2006; Bayram and Ayranci, 2010). Adsorption is a popular decolorization method due to its simplicity, availability and effectiveness in removing non-biodegradable pollutants (including dyes) from wastewater. Many adsorbents, such as activated carbon and biomass (Fernandez et al., 2010), have been investigated as dye-removing agents.

The commonly used adsorbent, activated carbon, has a good capacity for the removal of dyes (El Qada et al., 2008). Nevertheless, activated carbon is hard to regenerate and is expensive to apply, resulting in high costs. It is known that natural materials and some waste materials, classified as non-conventional low-cost adsorbents, have been used in dye-removal (Luo et al., 2010). For example, cheap, renewable and biodegradable cellulose-based materials, such as peanut hull, have often been used (Bhattacharyya and Sarma, 2003). Adsorbents used to remove pollutants, such as MB, from wastewater should simultaneously satisfy four requirements: ready availability, low price, convenient regeneration (if necessary) and good environmental safety profile.

Considering these four requirements, the use of inexpensive adsorbents based on solid wastes such as sawdust and tree leaves, to remove dyes from wastewaters, have been frequently studied in recent years (Crini, 2006). Yet, comparatively less attention has

* Corresponding authors. Tel./fax: +86 25 86881591.
E-mail addresses: yhwu@issas.ac.cn (Y. Wu), lzyang@issas.ac.cn (L. Yang).

0960-8524/$ - see front matter © 2011 Elsevier Ltd. All rights reserved.
doi:10.1016/j.biortech.2011.08.090

been focused on the removal of MB from wastewater through the use of agricultural solid wastes. Moreover, the adsorption processes in some studies are insufficiently described when using mathematic models, resulting in unclear understanding of the adsorption processes.

Sesame hull (SH), a readily available agro-based waste, may be an alternative for removing MB from wastewater. In this study, the detailed equilibrium and kinetics of MB adsorption by SH are investigated, in order to characterize the adsorption process.

The objectives of this study were: to determine whether MB in wastewater can be removed effectively by using SH; to determine the effects of specific parameters (pH, sorbent dosage, initial dye concentration, contact time and salt concentration) on the adsorption process; and to explain the adsorption of MB onto SH using mathematical isotherm models. The findings provide a promising and environmentally benign bioadsorbent for the removal of MB from wastewater. Additionally, this study helps to improve removal efficiency of MB and similar compounds using SH through modulating the aforementioned parameters.

2. Methods

2.1. The preparation of adsorbate (MB) and adsorbent (SH)

MB ($C_{16}H_{18}ClN_3S{\cdot}3H_2O$, C.I.52015, FW = 373.9, λ_{max} = 664 nm) was purchased from Sinopharm Chemical Reagent Co. LTD (Shanghai, China). The concentration of aqueous MB stock solutions for the following experiments was 1000 mg L^{-1}, diluted with water as required.

The dried sesame hull was collected in Shandong province, PR China. To remove water soluble materials, the hull was repeatedly washed with distilled water until the water became colorless and the washings and distilled water showed no absorbance difference. The hull was then filtered out and dried in an oven at 60 °C for 24 h. The dried material was crushed, sieved (pore, 250 μm) and activated at 110 °C for 2 h. The prepared SH powder was stored in an airtight container for the following experiments.

2.2. Batch adsorption experiments

The adsorption experiments were conducted in a batch system that was composed of some 100-mL Erlenmeyer flasks in a thermostatic shaker (30 °C, 200 rpm). Each flask was filled with 50 mL of solution and SH as appropriate. The following parameters were used in the series of adsorption experiments: pH from 2.50 to 10.50 (T = 30 °C, SH dose = 2.000 g L^{-1}, initial dye concentration = 200 mg L^{-1}), dye concentrations from 100 to 450 mg L^{-1} (T = 30 °C, SH dose = 2.000 g L^{-1}, pH 5.50), temperature from 10 to 40 °C (SH dose = 2.000 g L^{-1}, initial dye concentration = 200 mg L^{-1}, pH 5.50), contact time from 0 to 120 min (T = 30 °C, SH dose = 2.000 g L^{-1}, initial dye concentration = 200 mg L^{-1}, pH = 5.50), SH doses from 0.500 to 2.000 g L^{-1} (T = 30 °C, initial dye concentration = 200 mg L^{-1}, pH = 5.50) and salt (NaCl, $CaCl_2$ and $MgCl_2$) concentrations from 0 to 0.20 mol L^{-1} (T = 30 °C, SH dose = 2.000 g L^{-1}, initial dye concentration = 200 mg L^{-1}, pH = 5.50). To make a better description of the adsorption process, the initial MB concentrations were set between 100 and 450 mg L^{-1}.

The MB concentration was measured using the following process. Approximately 5 mL of MB solution was filtered through 0.45 μm membrane filters (the first 2 mL discarded), diluted (the absorbency values were adjusted to below 0.8 at 664 nm through controlling the dilution) and then measured using a UV–vis spectrophotometer (Shimadzu, UV2450, Japan). The amount of MB adsorbed onto SH at equilibrium was obtained using the following equation:

$$q_e = \frac{(C_0 - C_e)V}{M} \quad (1)$$

C_0 and C_e are the initial and equilibrium concentrations of dye (mg L^{-1}), respectively. V is the volume of the MB solution (L) and M is the amount of SH (g).

Scanning electron microscopy (SEM) (Sirion 200, FEI Co., Holland) was used to image the SH adsorbent before and after adsorption at a magnification of 3000×. The FTIR-PAS study (Nicolet 380, Thermo Electron Co., USA) was conducted using a spectral range of 4000–500 cm^{-1}.

2.3. Analysis and statistics

The equilibrium adsorption isotherms are of fundamental importance in the design of adsorption systems. In this study, three isotherm models were selected to describe the biosorption of MB onto SH at 30 °C. These isotherm models include the Langmuir, Freundlich and Temkin models, and adsorption intensity R_L (Eq. (2)) was also selected to describe the biosorption.

$$R_L = \frac{1}{1 + K_L C_0} \quad (2)$$

The R_L values indicate that the adsorption process is irreversible when R_L is 0, favorable when R_L is between 0 and 1, linear when R_L is 1, and unfavorable when R_L is greater than 1 (Wu et al., 2010).

To evaluate the kinetic mechanism that controls the adsorption process, the pseudo-first-order (Eq. (3)), pseudo-second-order (Eq. (4)) and intraparticle diffusion models (Eq. (5)) were used to interpret the experimental data.

$$\log(q_e - q_t) = \log q_e - \frac{k_1}{2.303} t \quad (3)$$

The variables q_e and q_t are the amount of dye adsorbed per unit mass of the adsorbent (mg g^{-1}) at equilibrium and at time t, and k_1 is the pseudo-first-order rate constant (min^{-1}). By plotting log ($q_e - q_t$) versus t, equilibrium uptake and pseudo-first-order rate constant can be determined.

$$\frac{t}{q_t} = \frac{1}{k_2 q_e^2} + \frac{t}{q_e} \quad (4)$$

The equilibrium rate constant (g (mg min)$^{-1}$) is given by k_2.

$$q_t = k_{id} t^{0.5} + C \quad (5)$$

The variable k_{id} is the intraparticle diffusion rate constant (mg g^{-1} $min^{-0.5}$) and C (mg g^{-1}) is the intercept. From the slope of the linear plot of q_t versus $t^{0.5}$, k_{id} can be evaluated.

The adsorption thermodynamic parameters were calculated according to the following equations (Thinakaran et al., 2008):

$$\log k_d = \frac{\Delta S^\circ}{2.303R} - \frac{\Delta H^\circ}{2.303RT} \quad (6)$$

$$K_d = \frac{C_a}{C_e} \quad (7)$$

$$\Delta G^\circ = -RT \ln K_d \quad (8)$$

In the above equations R is the universal gas constant (8.314 J mol^{-1} K^{-1}), ΔS° is standard entropy (J mol^{-1} K^{-1}), ΔH° is standard enthalpy (J mol^{-1}), ΔG° is the standard free energy (J mol^{-1}), K_d is the distribution coefficient for the adsorption, C_a is the amount of dye adsorbed of the solution at equilibrium (mg L^{-1}) and T is the solution temperature (K).

Each experiment was repeated three times and the mean results with error bar (±SD) were presented. All figures except SEM study were derived using MS Excel 2007.

3. Results and discussion

3.1. Characteristics of SH (before and after adsorption)

The SEM images for the SH adsorbent before and after adsorption are showed in Fig. 1S-a and S-b in the Supplementary, respectively. Before adsorption, the SH had a rough surface with heterogeneous pores and cavities, which indicated that there was a good possibility for MB to be trapped and adsorbed onto the surface because these pores and cavities provided a large exposed surface area. After adsorption, the surface of SH was comparatively smoother, implying that MB molecules might have become attached to the SH surface.

The FTIR-PAS spectral analysis is useful for identifying the functional groups on the surface of the SH powder and for determining which groups are responsible for the adsorption of MB molecules. The FTIR-PAS spectra of SH before and after adsorption as well as MB powder was recorded. The FTIR-PAS spectra in the range of 4000–500 cm^{-1} are shown in Fig. 1S-c in the Supplementary.

The FTIR-PAS spectra suggest that various functional groups detected on the surface are involved in the adsorption. The peaks observed around 1049, 1396, 1616, 2920 and 3390 cm^{-1} were significantly changed, which some peaks appeared red shift and the height of some peaks varied. These peaks can be attributed to C–O stretching, symmetric bending of CH_3, carbonyl group stretching, asymmetric and symmetric vibration modes of methyl and methylene groups and O–H stretching (Thinakaran et al., 2008), respectively. The polar functional groups, such as hydroxyl and carbonyl groups on the surface, are likely to provide adsorption capacity for SH adsorbents.

According to Fig. 1S-c in the Supplementary, besides the above-mentioned peaks, new peaks were also detected. For example, the spectrum of MB has an obvious peak at approximately 849 cm^{-1} because of the existence of Cl, and the spectrum of SH powder before adsorption showed no peaks nearby. After adsorption, however, a peak could be observed nearby on the spectrum of MB-contained SH, which confirmed that there was considerable MB attached onto the SH powder.

3.2. Effects of various conditions on adsorption

3.2.1. The Effect of pH on dye adsorption

At the initial MB concentration of 200 mg L^{-1} and the SH dosage of 2.000 g L^{-1}, the adsorption capacity of SH was investigated at pH values ranging from 2.50 to 10.50 at constant temperature (30 °C). Fig. 1a shows that the adsorption capacities were almost identical (90.99–92.11 mg g^{-1}) when the pH was changed from 3.54 to 9.58. The slightly higher adsorption capacity of SH at pH 10.50 (94.10 mg g^{-1}) may be attributed to the MB color loss in highly alkaline solutions (Fernandez et al., 2010). Conversely, the adsorption capacity decreased sharply at pH 2.50 (48.30 mg g^{-1}). Because the adsorption efficiency was not substantially influenced by the pH variation (when pH $\geqslant$ 3.54), all of the MB adsorption experiments were performed at 'natural' solution pH (approximately pH 5.50).

SH contains hydroxyl groups as well as carbonyl groups, as determined using FTIR-PAS. Therefore, the effect of pH on the adsorption of MB onto SH might be attributed to electrostatic attractions. Electrostatic attractions may operate over a large range of pH (here from pH 3.54 to pH 10.50) without having an effect on adsorption (Bhattacharyya and Sharma, 2005). At low pH values (pH < 3.54), the excessive H^+ ions competed with the dye cations (MB^+) for adsorption sites. At comparatively higher pH values (pH $\geqslant$ 3.54), the number of positively charged sites decreased and the number of negatively charged sites increased, causing the removal of this cationic dye.

3.2.2. Effect of adsorbent dosage on dye adsorption

Fig. 1b shows the effect of adsorbent dosage on the removal of MB (C_0 = 200 mg L^{-1}). It was found that the MB removal efficiency increased dramatically with increasing dosage up to 2.000 g L^{-1}. For higher doses, the removal efficiency remained fairly constant despite increases in the amount of SH. For an increase in SH dose from 0.500 to 8.000 g L^{-1}, the removal efficiency increased from 57.63% to 94.59%. The great efficiency increase from 57.63% to 91.65% occurred at doses from 0.500 to 2.000 g L^{-1}. However, as

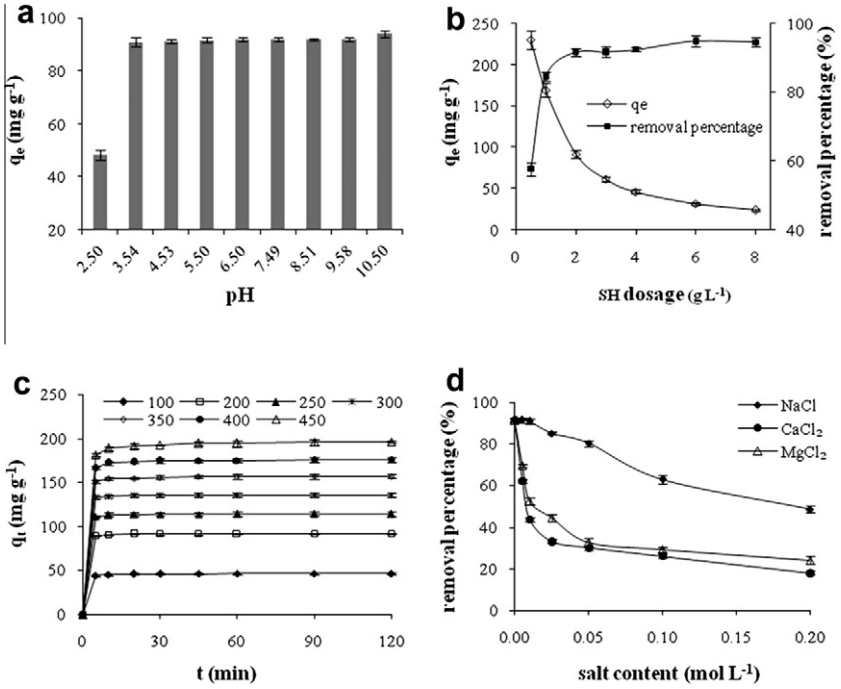

Fig. 1. The effects of operating parameters on the adsorption characteristics (agitation speed = 200 rpm). (a) Effect of solution pH on dye adsorption (C_0 = 200 mg L^{-1}, m = 2.000 g L^{-1}); (b) effect of adsorbent dose on dye adsorption (C_0 = 200 mg L^{-1}, m = 2.000 g L^{-1}); (c) effect of initial concentration and contact time on dye adsorption (V = 500 ml, m = 2.000 g L^{-1}); (d) effect of salt concentration on dye adsorption (C_0 = 200 mg L^{-1}, m = 2.000 g L^{-1}).

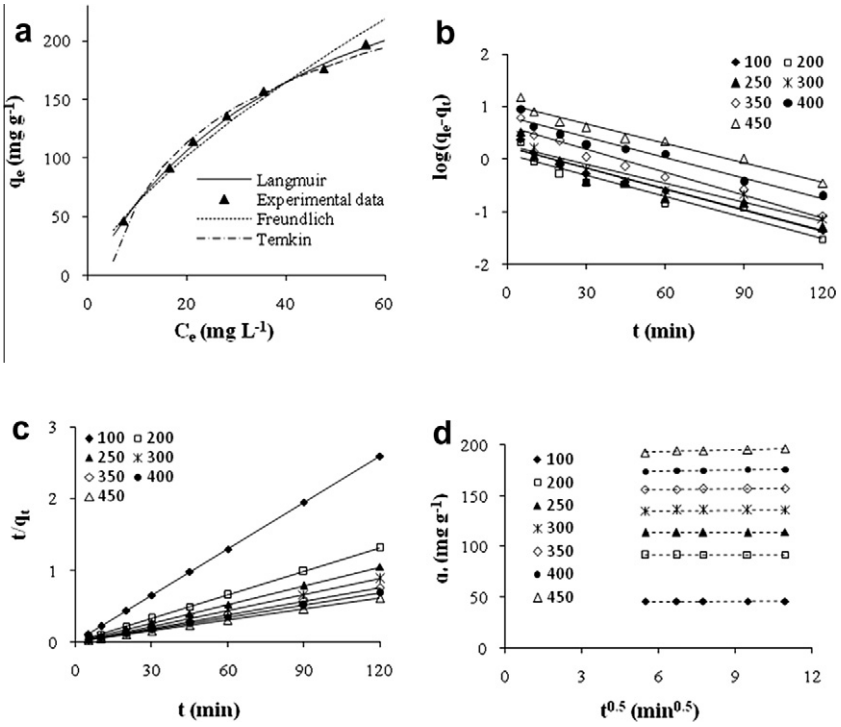

Fig. 2. (a) Langmuir, Freundlich and Temkin isotherm models for experimental data and plots of (b) pseudo-first-order (c) pseudo-second-order and (d) intraparticle diffusion (linear portions) kinetic models (experimental conditions: C_0 = 100, 150, 200, 250, 300, 350, 400 and 450 mg L^{-1}, SH dosage m = 2.000 g L^{-1}, temperature = 30 °C, agitation speed = 200 rpm).

the SH dosage increased from 2.000 to 8.000 g L^{-1}, the removal efficiency increased by only 2.94% (from 91.65% to 94.59%). It also has been found that (Fig. 1b) with the increase in the SH adsorbent dosage, the q_e decreased, from 230.51 mg g^{-1} (m = 0.500 g L^{-1}) to 23.65 mg g^{-1} (m = 8.000 g L^{-1}).

The initial dye concentration, adsorption sites and the available sorption surface provide the driving force to overcome the resistance to the mass transfer of dye between the aqueous and solid phases. The increase in adsorption sites and the available sorption surface enhance the interaction between adsorbent and MB, leading to the increase in MB removal efficiency. At every adsorption site, the amount of dye adsorbed per unit mass of adsorbent at equilibrium (q_e) decreases because the lower number of MB molecules means a 'less powerful driving force' favoring adsorption to the solid surface.

3.2.3. Effect of initial dye concentration and contact time on adsorption

The amount of dye adsorbed per unit mass of adsorbent at time t (q_t) increased with increasing dye concentration (Fig. 1c). The removal efficiencies declined from 92.79% to 87.50% (data not shown) when initial MB concentration increased from 100 to 450 mg L^{-1}. We observed a rapid increase of q_t to a constant value for each concentration being attained within 5 min.

The initial concentration of MB had little influence on the time needed to reach equilibrium. For all concentrations, the initial uptake of dye was rapid, indicating a rapid surface mass transfer between the aqueous (MB) and solid phases (SH). This indicates that the adsorption occurred mainly on the surface of the adsorbent. At higher initial concentrations (C_0 = 450 mg L^{-1}, for instance), the adsorption process could be divided into three stages. The first stage was fast as a result of the rapid attachment of MB to the surface of SH. The second stage occurred in the pores (intraparticle diffusion), which led to a slower attachment. In the third stage the adsorption process reached equilibrium. In this batch system, the removal rate of MB was controlled primarily by the rate of transport of MB from the exterior sites to the interior sites of SH particles, i.e., the removal rate was controlled by the second stage mentioned above.

It can be concluded that the concentration of dye will considerably affect the extent and rate of dye uptake onto the SH. The adsorption process mainly occurred in the first 5 min.

3.2.4. Effect of salt concentration on dye adsorption

Fig. 1d shows the effect of various concentrations of NaCl, $CaCl_2$ and $MgCl_2$ solutions on the amount of MB adsorbed per unit mass of SH for an initial MB concentration of 200 mg L^{-1} and SH dose of 2.000 g L^{-1}.

Table 1
MB adsorption capacity of some raw bioadsorbents reported in recent years.

Adsorbents	MB adsorption capacity (mg g^{-1})	Sources
Sesame hull	359.88	Present study
Guava leaf powder	295	Ponnusami et al. (2008)
Brazilian pine-fruit shell	252	Royer et al. (2009)
Palm kernel fibre	233.41	Ofomaja (2007)
Cupressus sempervirens cones	231.82	Fernandez et al. (2010)
Broad bean peels	192.7	Hameed and El-Khaiary (2008)
Tea waste	85.16	Uddin et al. (2009)
Luffa cylindrica fibers	49	Demir et al. (2008)
Yellow passion fruit	44.7	Pavan et al. (2008)
Olive pomace	42.3	Banat et al. (2007)
Hazelnut shells	41.3	Ferrero (2007)
Rice husk	40.58	Vadivelan and Kumar (2005)
Lemon peel	29	Kumar and Porkodi (2006)
Jute processing waste	22.47	Bulut and Aydın (2006)
Cereal chaff	20.3	Han et al. (2006)
Wheat straw	2.23	Batzias et al. (2009)

Table 2
Thermodynamic parameters for the adsorption of MB onto SH (experimental conditions: C_0 = 200, 400 mg L^{-1}, SH dosage m = 2.000 g L^{-1}, agitation speed = 200 rpm).

C_0 (mg L^{-1})	ΔH^0 (kJ mol^{-1})	ΔS^0 (kJ mol^{-1} K^{-1})	ΔG^0 (kJ mol^{-1})				R^2
			283.15 K	293.15 K	303.15 K	313.15 K	
200	−13.14	−23.48	−6.49	−6.24	−6.07	−5.76	0.9970
400	−12.83	−25.85	−5.37	−5.44	−5.04	−4.62	0.9287

It was found that the increase in salt concentration resulted in a decrease in MB adsorption onto SH. As the salt concentration increased from 0 to 0.20 mol L^{-1}, the removal efficiency decreased from 91.57% to 48.53%, 17.91% and 24.04% for NaCl, $CaCl_2$ and $MgCl_2$, respectively. This decrease could be attributed to the competitive effect between MB ions and salt cations for the sites available for the sorption process (Han et al., 2006). Alternatively, it is possible that as the ionic strength increased, the activity of MB and the active sites decreased, causing the adsorptive capacity for MB to decrease. It was theoretically expected that the effect of Ca^{2+} would be greater than that of Na^+ and Mg^{2+} due to its smaller hydrated radius and higher atomic number (Maurya et al., 2006).

3.3. Adsorption process

3.3.1. Equilibrium study

The theoretical adsorption isotherms are presented in Fig. 2a. Kinetic models and their parameters for the adsorption of MB onto SH are showed in Supplementary Table 1S. Experimental results obtained for MB adsorbed onto SH at 30 °C fit well to these three isotherm models. The equilibrium data were best represented by the Langmuir isotherm model and the plot between C_e/q_e and C_e yielded a straight line with a high correlation coefficient (R^2 = 0.9917).

According to the assumption of the Langmuir isotherm model, the adsorption of MB onto SH occurred as a monolayer on a surface that is homogenous in adsorption affinity. The maximum adsorption capacity of SH obtained using the Langmuir adsorption isotherm was 359.88 mg g^{-1}. When compared with previously reported bioadsorbents (Table 1) this suggests that SH has great potential as an adsorbent for methylene blue.

The R_L values for the adsorption of MB onto SH were in the range of 0.32–0.10 (data not shown) when the initial MB concentration varied from 100 to 450 mg L^{-1}. This indicates that the adsorption is a favorable process and that at higher initial MB concentrations, the adsorption is almost irreversible ($R_L \rightarrow 0$). Based on the Freundlich adsorption model, it was discovered that n = 1.43, indicating that MB adsorption onto SH is favored under this condition.

3.3.2. Adsorption kinetics

The kinetic models for MB adsorption onto SH are shown in Fig. 2b–d. When compared, the R^2 values for the pseudo-second-order kinetic model are higher than the pseudo-first-order kinetic model and the intraparticle diffusion model at all concentrations. This implies that the kinetic modeling of MB adsorbed onto SH closely followed the pseudo-second-order rate model. Additionally, it was deemed that a chemical process could be the rate-limiting step in the overall rate of the MB adsorption (Pan et al., 2011).

The intraparticle diffusion model was used to determine the rate-limiting step of the adsorption process. The plots did not pass through the origin despite the fact that the regression was linear (Fig. 2d). This indicates that intraparticle diffusion was not the only rate-limiting step (Yao et al., 2010). Meanwhile, k_{id} values (0.09 → 0.64) increased with increasing C_0 (100 → 450 mg l^{-1}), which indicates that high initial concentrations increased the driving force and promoted intraparticle diffusion of MB onto SH. The C values (45.44–189.73 mg g^{-1}) also increased with increasing C_0, which implies that the boundary layer diffusion effects increased with increasing initial MB concentration (Kannan and Sundaram, 2001).

3.3.3. Thermodynamic study

The negative values of ΔG^0 and ΔH^0 indicate that the adsorption process was feasible, spontaneous and exothermic (Table 2). This exothermic characteristic revealed that the adsorption process is more favored at lower temperatures. And the q_m increased with the temperature decreased, which had been confirmed by experiments. Furthermore, the ΔH^0 of physical adsorption is less than 40 kJ mol^{-1}, which suggests that the mechanism of MB adsorbed onto SH in this study is mainly a physical adsorption (Kara et al., 2003). The values of ΔG^0 obtained were within the ranges of −20 and 0 kJ mol^{-1}, which further confirmed that physical adsorption is the dominating adsorption mechanism (Mahmoodi et al., 2010).

4. Conclusion

Sesame hull (*Sesamum indicum* L.) was found to be suitable for removing hazardous synthetic dyes (i.e., methylene blue) by adsorption. The spontaneous, exothermic adsorption process attained equilibrium quickly, over a wide range of pH values. According to the Langmuir model, the maximum monolayer adsorption capacity of sesame hull was 359.88 mg g^{-1}. The adsorption kinetics were found to be best described by a pseudo-second-order reaction model. This study indicates that sesame hull, a readily-available, easily-deployed and environmental-friendly biomaterial, may be a promising non-conventional biosorbent for removing dyes from water.

Acknowledgements

This work was supported by the Innovative Project of Chinese Academy of Sciences (KZCX2-EW-QN401), the National Natural Science Foundation of China (41171363 and 41030640) and the Natural Science Foundation of Yunnan, China (2009CC006). The authors are grateful to Prof. Gangya Zhang and Miss Guiqin Zhou for the helps of SEM scanning and FTIR-PAS analyses, respectively.

Appendix A. Supplementary data

Supplementary data associated with this article can be found, in the online version, at doi:10.1016/j.biortech.2011.08.090.

References

Banat, F., Al-Asheh, S., Al-Ahmad, R., Bni-Khalid, F., 2007. Bench-scale and packed bed sorption of methylene blue using treated olive pomace and charcoal. Bioresour. Technol. 98, 3017–3025.

Batzias, F., Sidiras, D., Schroeder, E., Weber, C., 2009. Simulation of dye adsorption on hydrolyzed wheat straw in batch and fixed-bed systems. Chem. Eng. J. 148, 459–472.

Bayram, E., Ayranci, E., 2010. Electrochemically enhanced removal of polycyclic aromatic basic dyes from dilute aqueous solutions by activated carbon cloth electrodes. Environ. Sci. Technol. 44, 6331–6336.

Bestani, B., Benderdouche, N., Benstaali, B., Belhakem, M., Addou, A., 2008. Methylene blue and iodine adsorption onto an activated desert plant. Bioresour. Technol. 99, 8441–8444.
Bhattacharyya, K.G., Sarma, A., 2003. Adsorption characteristics of the dye, Brilliant Green, on Neem leaf powder. Dyes Pigments 57, 211–222.
Bhattacharyya, K.G., Sharma, A., 2005. Kinetics and thermodynamics of Methylene Blue adsorption on Neem (*Azadirachta indica*) leaf powder. Dyes Pigments 65, 51–59.
Bulut, Y., Aydın, H., 2006. A kinetics and thermodynamics study of methylene blue adsorption on wheat shells. Desalination 194, 259–267.
Crini, G., 2006. Non-conventional low-cost adsorbents for dye removal: a review. Bioresour. Technol. 97, 1061–1085.
Demir, H., Top, A., Balköse, D., Ülkü, S., 2008. Dye adsorption behavior of *Luffa cylindrica fibers*. J. Hazard. Mater. 153, 389–394.
El Qada, E.N., Allen, S.J., Walker, G.M., 2008. Adsorption of basic dyes from aqueous solution onto activated carbons. Chem. Eng. J. 135, 174–184.
Fernandez, M.E., Nunell, G.V., Bonelli, P.R., Cukierman, A.L., 2010. Effectiveness of *Cupressus sempervirens* cones as biosorbent for the removal of basic dyes from aqueous solutions in batch and dynamic modes. Bioresour. Technol. 101, 9500–9507.
Ferrero, F., 2007. Dye removal by low cost adsorbents: Hazelnut shells in comparison with wood sawdust. J. Hazard. Mater. 142, 144–152.
Ghosh, D., Bhattacharyya, K.G., 2002. Adsorption of methylene blue on kaolinite. Appl. Clay. Sci. 20, 295–300.
Hameed, B.H., El-Khaiary, M.I., 2008. Sorption kinetics and isotherm studies of a cationic dye using agricultural waste: broad bean peels. J. Hazard. Mater. 154, 639–648.
Han, R., Han, Y.W., et al., 2006. Removal of methylene blue from aqueous solution by chaff in batch mode. J. Hazard. Mater. B137, 550–557.
Ip, A.W.M., Barford, J.P., McKay, G., 2010. A comparative study on the kinetics and mechanisms of removal of Reactive Black 5 by adsorption onto activated carbons and bone char. Chem. Eng. J. 157, 434–442.
Kannan, N., Sundaram, M.M., 2001. Kinetics and mechanism of removal of methylene blue by adsorption on various carbons – a comparative study. Dyes Pigments 51, 25–40.
Kara, M., Yuzer, H., Sabah, E., Celik, M.S., 2003. Adsorption of cobalt from aqueous solutions onto sepiolite. Water Res. 37, 224–232.
Kumar, K.V., Porkodi, K., 2006. Relation between some two- and three-parameter isotherm models for the sorption of methylene blue onto lemon peel. J. Hazard. Mater. 138, 633–635.
Luo, P., Zhao, Y., Zhang, B., Liu, J., Yang, Y., Liu, J., 2010. Study on the adsorption of Neutral Red from aqueous solution onto halloysite nanotubes. Water Res. 44, 1489–1497.
Mahmoodi, N.M., Arami, M., Bahrami, H., Khorramfar, S., 2010. Novel biosorbent (Canola hull): surface characterization and dye removal ability at different cationic dye concentrations. Desalination 264, 134–142.
Maurya, N.S., Mittal, A.K., Cornel, P., Rother, E., 2006. Biosorption of dyes using dead macro fungi: effect of dye structure, ionic strength and pH. Bioresour. Technol. 97, 512–521.
Murugesan, K., Dhamija, A., Nam, I.-H., Kim, Y.-M., Chang, Y.-S., 2007. Decolourization of reactive black 5 by laccase: optimization by response surface methodology. Dyes Pigments 75, 176–184.
Ofomaja, A.E., 2007. Sorption dynamics and isotherm studies of methylene blue uptake on to palm kernel fibre. Chem. Eng. J. 126, 35–43.
Pan, J., Zou, X., Wang, X., Guan, W., Li, C., Yan, Y., Wu, X., 2011. Adsorptive removal of 2,4-dichlorophenol and 2,6-dichlorophenol from aqueous solution by β-cyclodextrin/attapulgite composites: equilibrium, kinetics and thermodynamics. Chem. Eng. J. 166, 40–48.
Pavan, F.A., Lima, E.C., Dias, S.L.P., Mazzocato, A.C., 2008. Methylene blue biosorption from aqueous solutions by yellow passion fruit waste. J. Hazard. Mater. 150, 703–712.
Ponnusami, V., Vikram, S., Srivastava, S.N., 2008. Guava (*Psidium guajava*) leaf powder: novel adsorbent for removal of methylene blue from aqueous solutions. J. Hazard. Mater. 152, 276–286.
Royer, B., Cardoso, N.F., Lima, E.C., Vaghetti, J.C.P., Simon, N.M., Calvete, T., Veses, R.C., 2009. Applications of Brazilian pine-fruit shell in natural and carbonized forms as adsorbents to removal of methylene blue from aqueous solutions – kinetic and equilibrium study. J. Hazard. Mater. 164, 1213–1222.
Sharma, P., Kaur, R., Baskar, C., Chung, W.-J., 2010. Removal of methylene blue from aqueous waste using rice husk and rice husk ash. Desalination 259, 249–257.
Thinakaran, N., Panneerselvam, P., Baskaralingam, P., Elango, D., Sivanesan, S., 2008. Equilibrium and kinetic studies on the removal of Acid Red 114 from aqueous solutions using activated carbons prepared from seed shells. J. Hazard. Mater. 158, 142–150.
Uddin, M.T., Islam, M.A., Mahmud, S., Rukanuzzaman, M., 2009. Adsorptive removal of methylene blue by tea waste. J. Hazard. Mater. 164, 53–60.
Vadivelan, V., Kumar, K.V., 2005. Equilibrium, kinetics, mechanism, and process design for the sorption of methylene blue onto rice husk. J. Colloid. Interf. Sci. 286, 90–100.
Wu, Y., He, J., Yang, L., 2010. Evaluating adsorption and biodegradation mechanisms during the removal of microcystin-RR by periphyton. Environ. Sci. Technol. 44, 6319–6324.
Yao, Y., Xu, F., Chen, M., Xu, Z., Zhu, Z., 2010. Adsorption behavior of methylene blue on carbon nanotubes. Bioresour. Technol. 101, 3040–3046.